SLAC-PUB-1115
(TH)and (EXP)
August 1972

EMPIRICAL OBSERVATION ON THE ENERGY DEPENDENCE OF VARIOUS PARTICLE CROSS SECTIONS†

F. Martin

Stanford Linear Accelerator Center
Stanford University, Stanford, California 94305

ABSTRACT

The energy dependence of total cross sections and total elastic cross sections have been examined for protons, anti-protons, kaons, pions and photons. This dependence is very well expressed in terms of the center of mass velocity $\beta = 2\ P^*/\sqrt{s}$. Some comments are made on the relationship to Regge theory.

† Work supported by the U. S. Atomic Energy Commission.

(Submitted to Phys. Rev.)

I. Introduction

A good deal of speculation on what happens to the collision cross sections of protons, kaons, and pions at ultra high energies has been issued out over the past decade.[1] Now that we are on the verge of achieving some measurements at laboratory energies in excess of 200 GeV/c the subject has become even more intriguing. In this paper we observe that the asymptotic behavior of many cross sections can be expressed quite precisely as a simple function of $\beta = 2P^*/\sqrt{s}$ where P^* is the initial center-of-mass momentum and s is the square of the invarient mass. The momentum range over which this variable applies seems to be for laboratory momenta greater than 2.5 GeV/c.

The processes examined are the total scattering and the total elastic scattering cross sections for protons, anti-protons, kaons, pions, and photons on protons. In addition to these, the real-to-imaginary amplitudes in elastic scattering, for protons and pions, the $\pi^- p \rightarrow \pi^o n$ charge exchange, the slope of the differential elastic scattering for protons and K^+, and the differential elastic scattering of protons at 90° in cm have been scrutinized.[2]

In general the functional dependence for cross sections takes the form:

$$\sigma = \frac{A}{\beta^n}\left(1 + C\sqrt{1-\beta^2}\right)^2$$

and

$$\lim_{s \to \infty} \sigma = A\frac{1}{\beta^n}\left(1 + C\sqrt{\frac{2M^2}{s}}\right)^2 = A\left(1 + \frac{2nM^2}{s} - \frac{n\Delta^2}{s^2}\right)\left(1 + 2C\sqrt{\frac{2M^2}{s}}\right)$$

Where

$$M^2 = \text{Mass}^2\ (\text{beam}) + \text{Mass}^2\ (\text{target})$$

$$\Delta = \text{Mass}^2\ (\text{beam}) - \text{Mass}^2\ (\text{target})$$

The values that n takes on seem to be either integer or half integer numbers.

We can compare this equation to the energy dependence of the Pomeron Regge trajectory. Using the optical theorem and the simple expansion of the Regge amplitude we find:

$$\sigma_T \alpha \frac{1}{\beta s} \left(\cos \theta_t\right)^{\alpha_p(t)} \Big|_{t=0} \underset{s\to\infty}{=} \lim \frac{1}{\beta s} \left(s - M^2\right) \simeq 1 + \frac{M^2}{s}$$

From kinematics alone the Pomeron has an s dependence similar to that observed here, but it falls too rapidly with s. The "C" parameter consequently represents, if you wish, the additional Regge trajectories required to describe the cross section. The energy dependence of this term is not easily deduced from Regge theory. Moreover, most Regge theories predict positive values for "C" for both particle and anti-particle cross sections. Our fits to the data do not find this to be uniformly true, consequently, several cross sections seem to approach their asymptotic values from below.

Although it would be premature, to say the least, to attach any theoretical interpretation to this circumstance, three possibilities suggest themselves:

1. This variable serves as a very convenient method for comparing cross sections measured in different experiments and for extrapolating between and beyond existing measurements.

2. It provides a convenient function for comparing the data with

the various theoretical models that predict these cross sections. For example, the measured K^-p/K^+p total cross sections seem to be well represented when $C = \pm .217$ and $n = 1.0$. Thus given our present knowledge of this data, we conclude that a Pomeron plus equal amounts of odd parity exchange in the two processes accounts for the observed cross sections and that other exchanges are unnecessary.

3. At the risk of being naive, one concludes from this experience that there ought to exist a simple interpretation of high energy cross sections, one involving just relativistic behavior of moving objects. Moreover, any complex model conjured up to describe high energy behavior must somehow reduce numerically to the functions described here.

The Method

The scattering data was analyzed in two ways. First we use a straightforward procedure of fitting a given cross section to:

$$\sigma = A\beta^n \qquad (1)$$

The "A" and "n" were fitted together and then an appropriate integer or half integer value for "n" was chosen and "A" refitted. The results of these fits are presented in Table 1 and shown graphically along with the data as dashed lines.

Also tabulated are the number of data points used in the fits and the dates up to which time the data was collected. The "RelX^2 is defined as:

$$\text{Rel}X^2 = \left[\sum_{\text{data}} (\text{DATA-FIT})^2/\text{error}^2/(\text{degrees of freedom}) \right]^{\frac{1}{2}}$$

The error for each data point was used and when available the normalization error was added to the statistical error in the standard

procedure, but no error on the momentum was used. Qualitatively, the systematic variations between experiments appears to be the principal source of uncertainty in the fits.

This fitting results in considerable violation of the Pomeranchuk theorem. The asymptotic limit of the cross sections for particle and anti-particle interactions are many standard deviations apart. To investigate this discrepancy the following functions were used:

$$\sigma\ (\text{particle} - p) = A\beta^n \left(1 + C\sqrt{1-\beta^2}\right)^2$$

$$\sigma\ (\text{anti-particle} - p) = A\beta^n \left(1 + \bar{C}\sqrt{1-\beta^2}\right)^2 \qquad (2)$$

These functions were fitted simultaneously for A, C, $\bar{C}$ with n fixed and adjustable. The results are presented in Table 2 and shown graphically as the solid lines in the figures.

The Proton and Anti-Proton Data

The collected proton and anti-proton data[4] are presented in Figs. 1, 2, and 3. For the total cross sections, Fig. 1, we see from Table 1 that the proton and anti-proton cross sections have quite different asymptotic values when fit individually. In order to satisfy the Pomeranchuk theorem some odd parity component must be added. The "ideal" fit is indistinguishable from the "best" fit and we find that about 16% of the proton amplitude and 25% of the anti-proton amplitude is represented by other trajectories. The fact that the proton component is about half the anti-proton component suggests some concelling takes place in the proton interaction. Also the annihilation cross section is not explicit-

ly included in the functions and must manifest itself through the $\bar{C}$ parameter.

Muirhead and Poppleton [5] have studied the behavior of the annihilation process $\bar{p}p \rightarrow n\pi$, but at high energies their analysis leads to awkward results. For the various multi-pion channels they extracted the matrix element by dividing the cross section by the n-pion phase space. They observed that the matrix element had the following s dependence:

$$\left|T_{fi}\right|^2 = An\ s^{-5}$$

where An is a constant for any value of n. If we ignore the pion mass, at high energies, the annihilation cross section becomes:

$$\sigma_A = \frac{(2\pi)^4 M^2}{p\sqrt{s}}\ s^{-5} \sum_{n=2}^{\infty} \frac{\left(A_e^n + A_o^n\right) s^{n-2}}{(n-2)!\ (n-1)!}$$

Here A_e and A_o refer to n even or odd, respectively. This expression for σ_A increases rapidly with energy beyond a laboratory energy of 50 GeV/c. The anti-proton function clearly needs some additional factors in the energy dependence in order to fit the data, and more data on the annihilation cross section would provide some clue as to the nature of the energy dependence.

Other features of this fit suggest that because the exchange is negative, the total proton cross section must rise and approach the asymptotic value from below. Recent measurements of elastic scattering data from the ISR gives total cross sections varying from 37.0 to 40.3 mb [6] with errors of 1.5 to 2.0 mb. The inclusion of these measurements in the fits produced results identical to those in Table 2 where they are not represented. Thus, they are consistent with the suggested violation of duality although the Serpukhov data [4] does not

indicate an increase which ought to commence around a laboratory momentum of 20 GeV/c for 16% odd parity. Also, as these fits now stand, the sum of $\sigma_T(pp) + \sigma_T(\bar{p}p)$ cannot rise because the sum of $C + \bar{C}$ is positive. Finally, Fig. 2 shows earlier measurements of $\sigma_T(pp)$ in the low energy region. It is difficult to believe that the precision of the function is merely a coincidence.

Figure 3a shows how the elastic cross section behaves and again we see that the anti-proton data requires considerable odd parity exchange whereas the proton data is consistent with no such exchange.

Figure 3b shows how the slope of the elastic scattering[7] is evaluated. The exponent of β is clearly consistent with that for the elastic cross section. To conserve space, the highest energy point from the ISR (1500 GeV/c in the laboratory) is shown at p_{Lab} equal 1000 GeV/c[8]. The considerable scatter observed in the data may well come from the difficulty in defining the slope of the cross section. This number varies according to the range of t used and whether one includes a t^2 term in the determination.

Figure 4 shows how the real-to-imaginary part of scattering amplitude[7] fits the form $.74\sqrt{1-\beta^2}$.

It has been postulated that the differential elastic cross section will equal the fourth power of electric form factor as s approaches infinity.[9] If this is so and the t dependence of elastic scattering is scaled by β^n as suggested by the energy dpendence of the slope then perhaps we should find that:

$$\left.\frac{d\sigma}{dt}\right|_{\theta\ cm=90^\circ} \propto \frac{1}{\left(1 + \frac{\beta^n t}{.71}\right)^8}$$

The results of this fit are shown in Fig. 5 with n=2. Quantitatively, the fit is unsatisfactory, but the qualitative trend is similar to the data. Recently, Gunion, Brodsky and Blankenbecler[10] have analyzed this cross section in terms of a parton model and arrive at a functional form, in the limit as s goes to infinity, of:

$$\left.\frac{d\sigma}{dt}\right|_{\theta\ cm=90^{o}} \propto \frac{1}{s^{12}}$$

When the p_{Lab} is greater than 10 GeV/c this fits the data very well. Unfortunately, the data above 10 GeV/c is inadequate to make a conclusive selection among the various interpretations.

The Pion Data

The enormous quantity of total cross section data[4] provides us with sufficient information to obtain quite detailed descriptions of the process, Fig. 6a and 6b.

The two fits for the total pion cross sections give somewhat different results. Following the pattern for protons, and also for kaons, we have set n=-1.0. The exchange parameter has the same sign for both π^+ and π^-, but the magnitude for the negative pion is twice that of the positive pion. On the other hand if n decreases to -1.5 we find that the π^+ cross section is well represented with C=0. The two fits are indistinguishable and we note that in both cases the cross sections approach the asymptotic value from above; for consistancy we choose n=-1.0. The sum of $\sigma_t(\pi^+p)$ + $\sigma_t(\pi^-p)$ will also rise as s increases because the sum $C + \bar{C}$ is less than zero. The details of the low momentum region are shown in Figs. 6c and 6d, and again indicate a remarkable precision for these functions.

Figure 7 shows the behavior of the elastic scattering data. The data, although not copious, indicates about 4% odd parity exchange for both π^+ and π^- scattering. Also the large value for n indicates that the cross section approaches its asymptotic value at low energies and is very flat for p_{Lab} greater than 20 GeV/c. For n=-3.0 the exchange parameter is quite large, but in both cases it is positive and the two cross sections remain larger than the asymptotic value.

If the π^+/π^- cross sections are well represented by I_t=0 and ω or ρ type exchanges then we ought to see a correlation between these components of the total and elastic cross sections on one hand and the charge exchange cross section $\sigma(\pi^- p \rightarrow \pi^o n)$ on the other hand.[11] Figure 8 shows a fit of this cross section to:

$$\sigma(\pi^- p \rightarrow \pi^o p) = .486\ (1-\beta^2)/\beta^3$$

The odd parity amplitude in the total cross section data predicts a scale factor of .35 which compares favorably with the above formula; although the energy dependence of this process identifies with the odd parity component in elastic scattering.

Figure 9 shows the energy dependence of the real-to-imaginary amplitude as a function of $\sqrt{1-\beta^2}$. The high energy points in the π^+ plot are the calculated values from a recent Serpukhov paper[4] on total cross sections and the scale factor is .65 for π^+ and .52 for π^-.

The Kaon Data

Figures 10a,b,c and d show the details of total and elastic scattering for kaons on hydrogen. There is little to say here that has not already been covered in the previous discussions. The 22% of odd parity

exchange in the total cross section accounts very well for the k^+ total cross section. The data strongly suggest that duality is not satisfied for these reactions. The "ideal" and "best" fits in both processes are indistinguishable. And it may be that the sum $\sigma_t(k^+p) + \sigma_t(k^-p)$ decreases to its asymptotic value.

The Total Photoabsorption Data[12]

This cross section along with a simple fit to $\beta^{-1.0}$ is shown in Fig. 11. We observe only that the energy dependence is identical to that of the other cross sections in the asymptotic limit.

Summary

This parameterization seems to be a very concise method of describing the energy dependence for many cross sections with the possible exception of anti-proton data. Although it may be merely a coincidence, the precision of the fits to the data seems quite remarkable. On the other hand we have no theory for this formulation. We can also observe that the exponent of β seems to be limited to -1.0 for the total cross sections and -3.0 for the elastic cross sections.

If we interpret the "C" parameter as representing other trajectories or exchange contributions to the total cross sections then the pion and kaon total cross sections are well represented by such mechanisms, although the k^+ cross section violates duality. The anti-proton system is more complex. The extrapolated values for proton and anti-proton cross sections as shown in Table 1 are much further apart than for the other processes. It suggests that we need to know more about the anti-proton annihilation cross section or possibly the Pomeranchuk theorem may not be correct for this reaction.[13]

Acknowledgements

I am grateful for the many suggestions from R. Blankenbecler, J. Gunion and M. L. Perl for his support. This work was started while I was visiting CERN and I wish to thank L. Montanet for his support.

REFERENCES

1. Proceedings of the Lund Conference on Elementary Particles, June 25, 1969. Reviews by L. Dilella, D. R. O. Morrison, L. Monanet, and E. Lillithun. The International Conference on High Energy Physics at Kiev 1970, for example Tai Tsun Wu and Hung Cheng. For an earlier Regge approach see V. Barger, M. Olsson and D. D. Reeder, Nuclear Physics B5, 411 (1968).
2. Except where cited the data were obtained from the various data summaries compiled by the "Particle Data Group" of Lawrence Radiation Laboratory and collaborators and published in the UCRL 20000 series. Also "compilation of Cross Sections" of several classes by E. Flaminio, J. D. Hansen, D. R. O. Morrison, N. Tovey, published in the CERN-HERA Reports.
3. For a discussion of this phenomenon see: "Two-body Hadron-Hadron Interactions" by C. Michael; presented at the IVth International Conference on High Energy Collisions held at Oxford, April 1, 1972.
4. S. P. Denisov et al., Physics Letters 36B, 528 (1971) and Physics Letters 36B, 415 (1971).
5. H. Muirhead, A. Poppleton, Physics Letters 29B, 448 (1969).
6. M. Holder et al., Physics Letters, 35B, 361 (1971). Results from the "ACHGT" and "CERN-ROMA" groups. Presented at the 16th International Conference on High Energy Physics by Hugo Maldi.
7. Kh. M. Chernev et al., Physics Letters 36B, 266 (1971).
8. M. Holder et al., Physics Letters 35B, 355 (1971) and U. Amaldi et al., Physics Letters 36B, 504 (1971).
9. T. T. Wu and C. N. Yang, Phys. Rev. 137B, 708 (1965). H. Barbanel, S. Drell and F. Gilman, Phys Rev. Letters 20, 280 (1968).
10. J. F. Gunion, S. J. Brodsky and R. Blankenbecler SLAC-PUB-1037,

April 1972; submitted to Physics Letters.

11. V. N. Bolotov et al., Physics Letters 38B, 120 (1970).

12. D.W.G.S. Leith, "Rho Meson Photoproduction from Complex Nuclei". Invited talk at the Third International Conference on High Energy Physics and Nuclear Structure. Also SLAC-PUB-679, September 1969.

13. "Remarks About the Pomeranchuk Theorem" by André Martin, presented at the Stony Brook Conference on High Energy Collisions held in September, 1969.

TABLE 1

Results of fitting the cross sections to $A \cdot \beta^n$ with n fixed and variable. These are shown as dashed lines on the data plots.

Beam		Proton		Anti-Proton		K^+		K^-		π^+		π^-		Gamma	
	n	-.5	-.52	-2.0	-1.8	0	.03	-2.0	-2.1	-2.0	-1.4	-2.0	-2.0	-1.0	-1.4
Total	A	37.8	37.6	41.8	43.8	17.5	17.5	19.9	19.8	22.0	23.1	24.1	24.1	115.0	111.3
Cross	Rel χ^2	3.6	3.5	3.3	2.5	2.1	2.1	1.1	1.1	4.1	2.2	1.3	1.3	1.1	1.0
Section	Data	76	76	61	61	62	62	35	35	159	159	182	182	65	65
	Date	Nov.	1971	June	1972	Nov.	1971	Nov.	1971	Nov.	1971	Nov.	1971	Dec.	1970
Total	n	-3.0	-2.90	-3.0	-2.98	-2.0	-2.1	-3.0	-3.89	-4.0	-4.8	-4.0	-4.0		
Elastic	A	7.16	7.26	9.36	9.41	3.10	3.06	2.79	2.49	4.01	3.67	3.80	3.76		
Cross	Rel χ^2	1.7	1.7	1.6	1.6	.4	.4	1.8	.71	1.1	.9	1.2	1.2		
Section	Data	35	35	15	15	8	8	15	15	19	19	36	36		
	Date	May	1972	June	1972	Dec.	1970	Dec.	1970	Dec.	1970	Dec.	1970		
Slope of	n	3.0	2.7			3.0	3.7								
The	A	11.8	11.6			6.76	7.2								
Differential	Rel χ^2	2.6	2.5			1.2	1.0								
Cross	Data	70	70			9	9								
Section	Date	July	1972			Dec.	1970								

TABLE 2

Results of fitting the particle and anti-particle proton cross section to $A\beta^n\left(1 + C\ (\bar{C})\ \sqrt{1-\beta^2}\right)^2$. These are shown as solid lines on the data plots.

Beam		Proton/Anti-Proton		K^+/K^- - Proton		π^+/π^- - Proton	
		Ideal	Best	Ideal	Best	Ideal	Best
	Exponent, N	-1.0	-.83 ± .007	-1.0	-1.04 ± .1	-1.0	-1.5 ± .06
Total	A	41.3 ± .04	39.8 ± .08	19.2 ± .05	19.3 ± .1	22.4 ± .03	23.1 ± .08
Cross	C	-.164 ± .0007	-.103 ± .003	-.246 ± .003	-.253 ± .018	.103 ± .003	.002 ± .011
Sections	$\bar{C}$	.248 ± .0009	.329 ± .004	.143 ± .007	.135 ± .021	.229 ± .003	.123 ± .011
	Rel χ^2	4.8	4.5	1.3	1.3	1.3	1.2
	Exponent, N	-3.0	-3.0	-3.0	-3.0	-4.0	-3.0
Total	A	8.03 ± .13	7.4 ± .13	2.74 ± .05	2.35 ± .13	3.87	3.42 ± .16
Elastic	C	-.121 ± .007	-.035 ± .020	-.031 ± .020	.186 ± .079	.040 ± .015	.341 ± .076
Cross	$\bar{C}$	.121 ± .007	.212 ± .020	.031 ± .020	.206 ± .066	-.040 ± .015	.247 ± .071
Sections	Rel χ^2	1.94	1.8	1.0	.82	1.1	1.1

FIGURE CAPTIONS

1. The total cross sections for protons (lower curve) and anti-protons (upper curve) on protons. For this and all of the subsequent figures the significant error bars are shown, otherwise they are contained in the spot size and the curves are described in the text and the tables.
2. The low momentum detail of the total proton-proton cross section.
3. (a) The total elastic scattering cross sections for protons (lower curve) and anti-protons (upper curve) on protons.

   (b) The slope of the proton elastic scattering cross section.
4. The ratio of the real to imaginary parts of the forward scattering amplitude for protons.
5. The $d\sigma/dt$ scattering for protons measured at 90^{o} in the center of mass.
6. (a) Total cross sections for π^{+} on protons.

   (b) Total cross sections for π^{-} on protons.

   (c) A detail of the total cross sections for π^{-} at low momenta.

   (d) A detail of the total cross sections for π^{+} at low momenta.
7. The elastic scattering cross sections for π^{+} (upper curve) and π^{-} (lower curve) on protons.
8. The $\pi^{-}p \rightarrow \pi^{o}n$ charge exchange cross section.
9. The ratio of the real to imaginary parts of the forward scattering amplitude for π^{+} (upper curve) and π^{-} (lower curve).
10. (a) Total cross sections for K^{-}(upper curve) and K^{+} (lower curve) on protons.

    (b) The total elastic scattering cross section for K^{+} on protons.

    (c) The total elastic scattering cross section for K^{-} on protons.

    (d) The slope of the elastic scattering cross section for K^{+}.
11. The total photo absorption cross section.

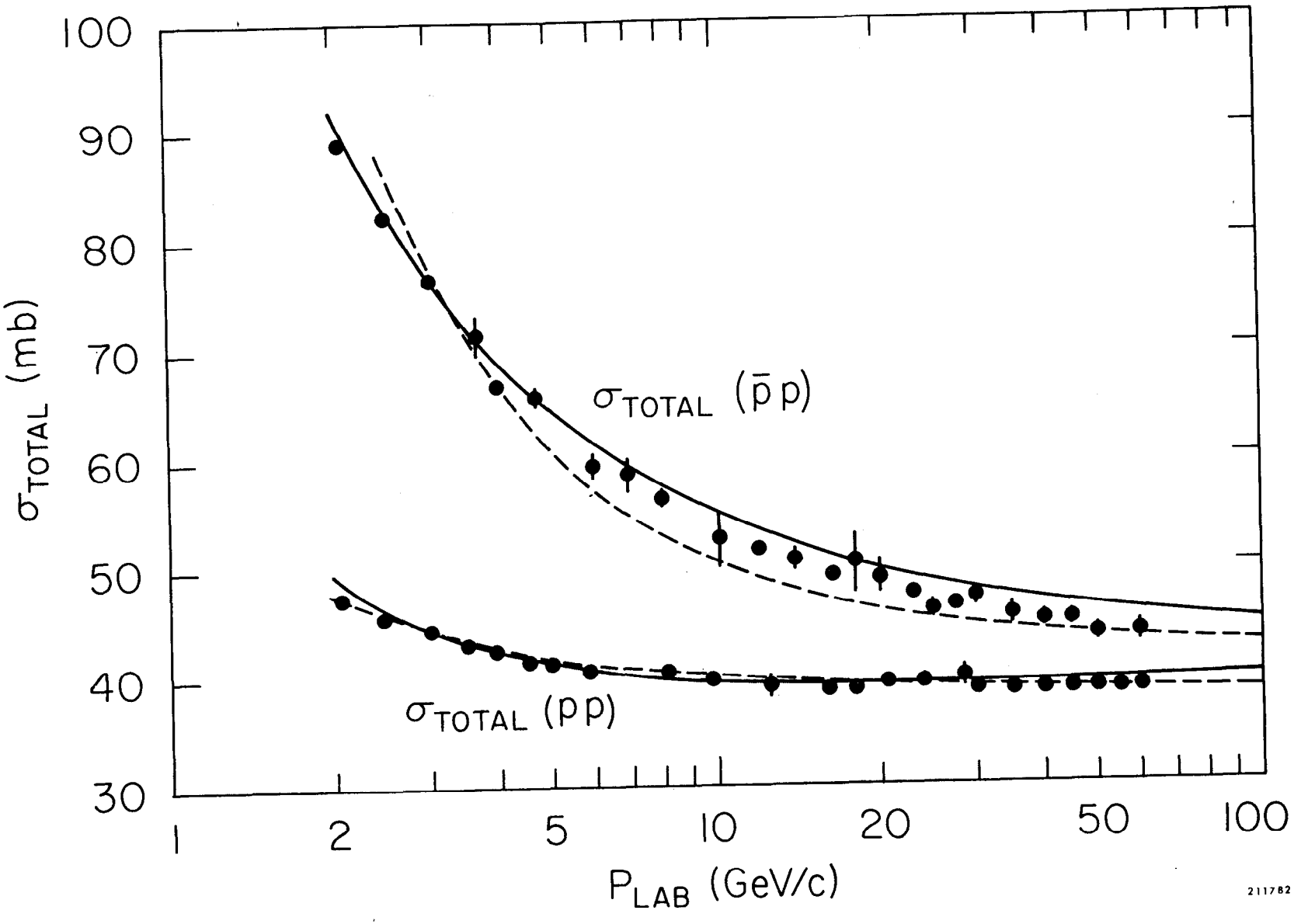
100
90
80
70
60
50
40
30
σ_{TOTAL} (mb)
σ_{TOTAL} ($\bar{p}$ p)
σ_{TOTAL} (p p)
1
2
5
10
20
50
100
P_{LAB} (GeV/c)
211782

FIG. 1

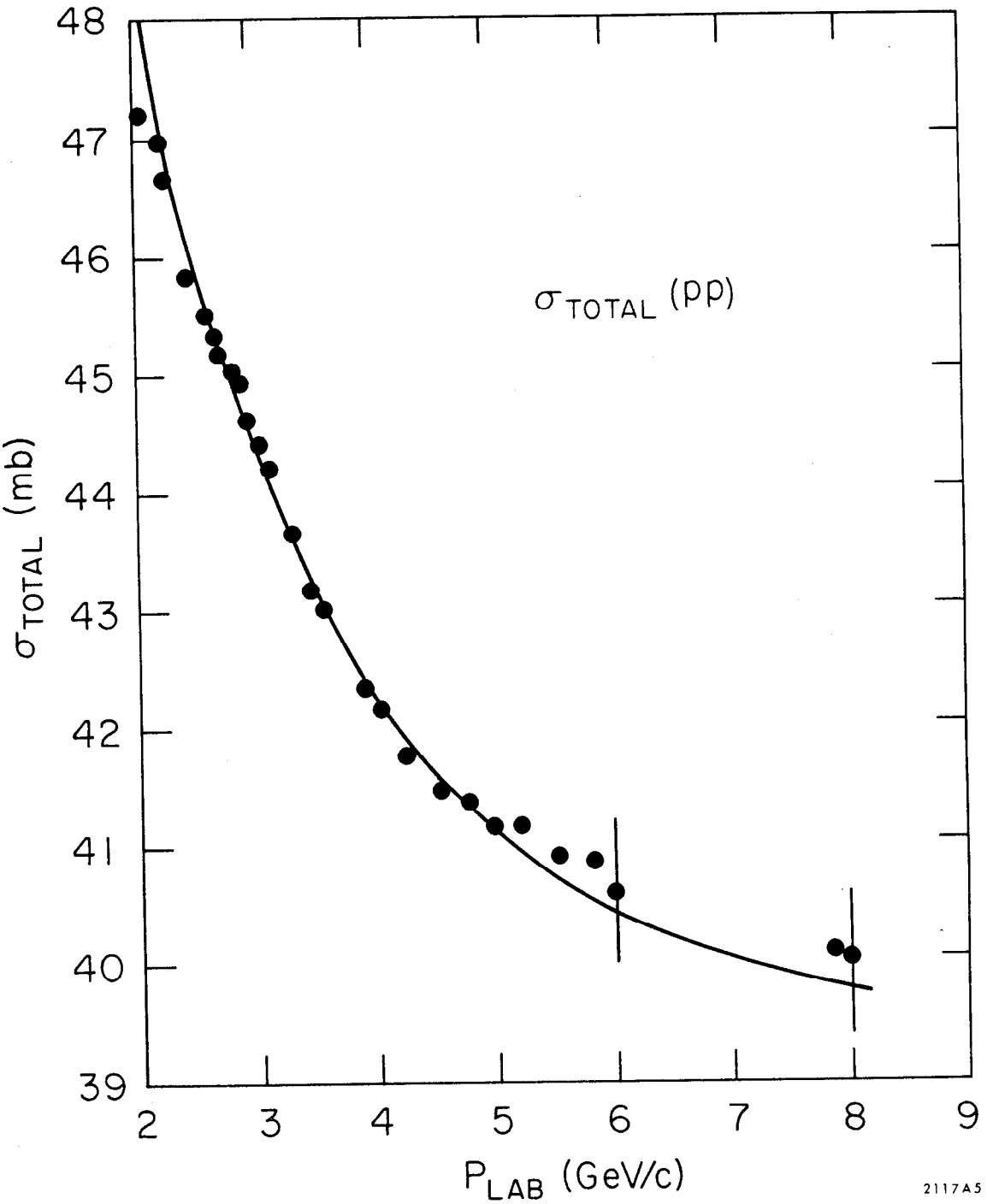
48
47
46
45
44
43
42
41
40
39
2
3
4
5
6
7
8
9
σ TOTAL (mb)
P LAB (GeV/c)
σ TOTAL (pp)
2117A5

FIG. 2

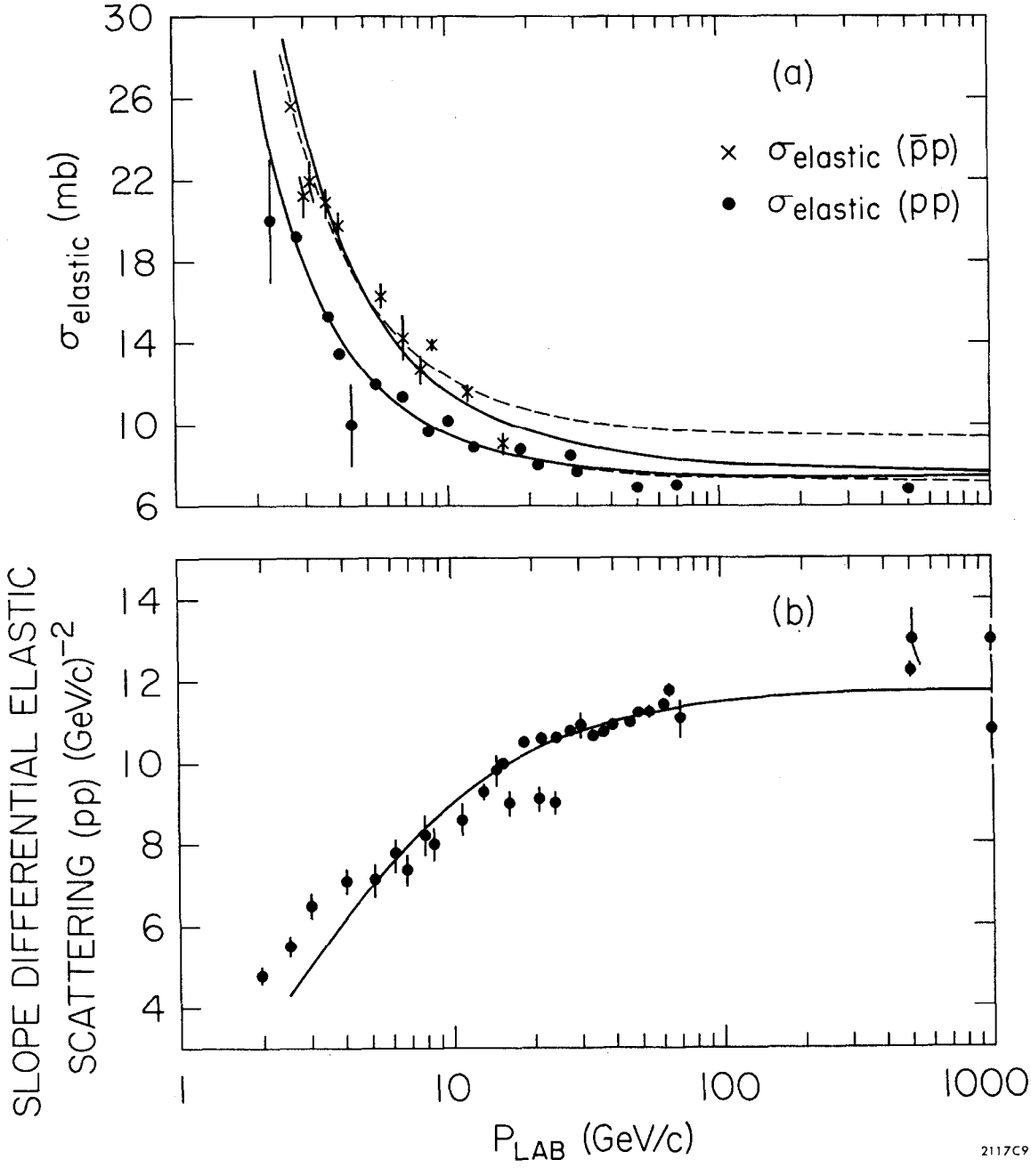
30
26
22
18
14
10
6
$\sigma_{elastic}$ (mb)
(a)
× $\sigma_{elastic}$ ($\bar{p}p$)
• $\sigma_{elastic}$ (pp)
14
12
10
8
6
4
SLOPE DIFFERENTIAL ELASTIC SCATTERING (pp) (GeV/c)$^{-2}$
(b)
1
10
100
1000
P_{LAB} (GeV/c)
2117C9

FIG. 3

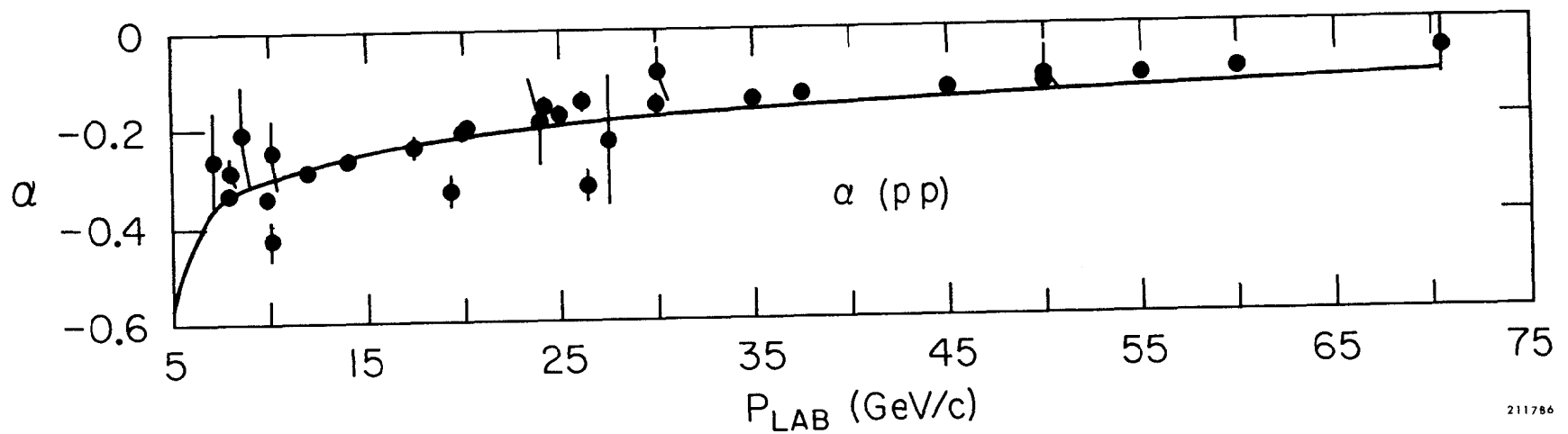

FIG. 4

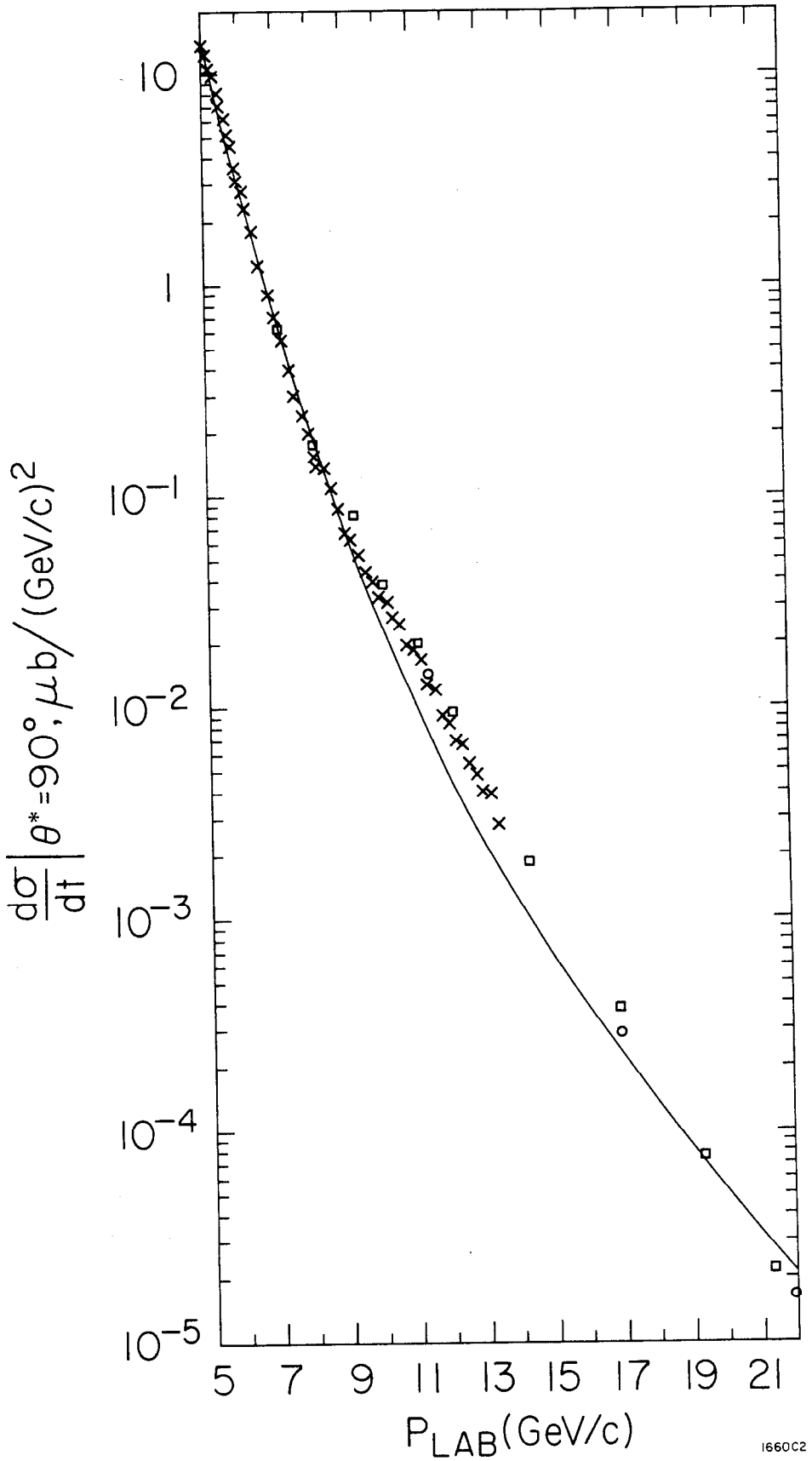
10
1
10^{-1}
10^{-2}
10^{-3}
10^{-4}
10^{-5}
$\frac{d\sigma}{dt}\Big|_{\theta^*=90°}$, $\mu b/(GeV/c)^2$
5 7 9 11 13 15 17 19 21
P_{LAB}(GeV/c)
1660C2

FIG. 5

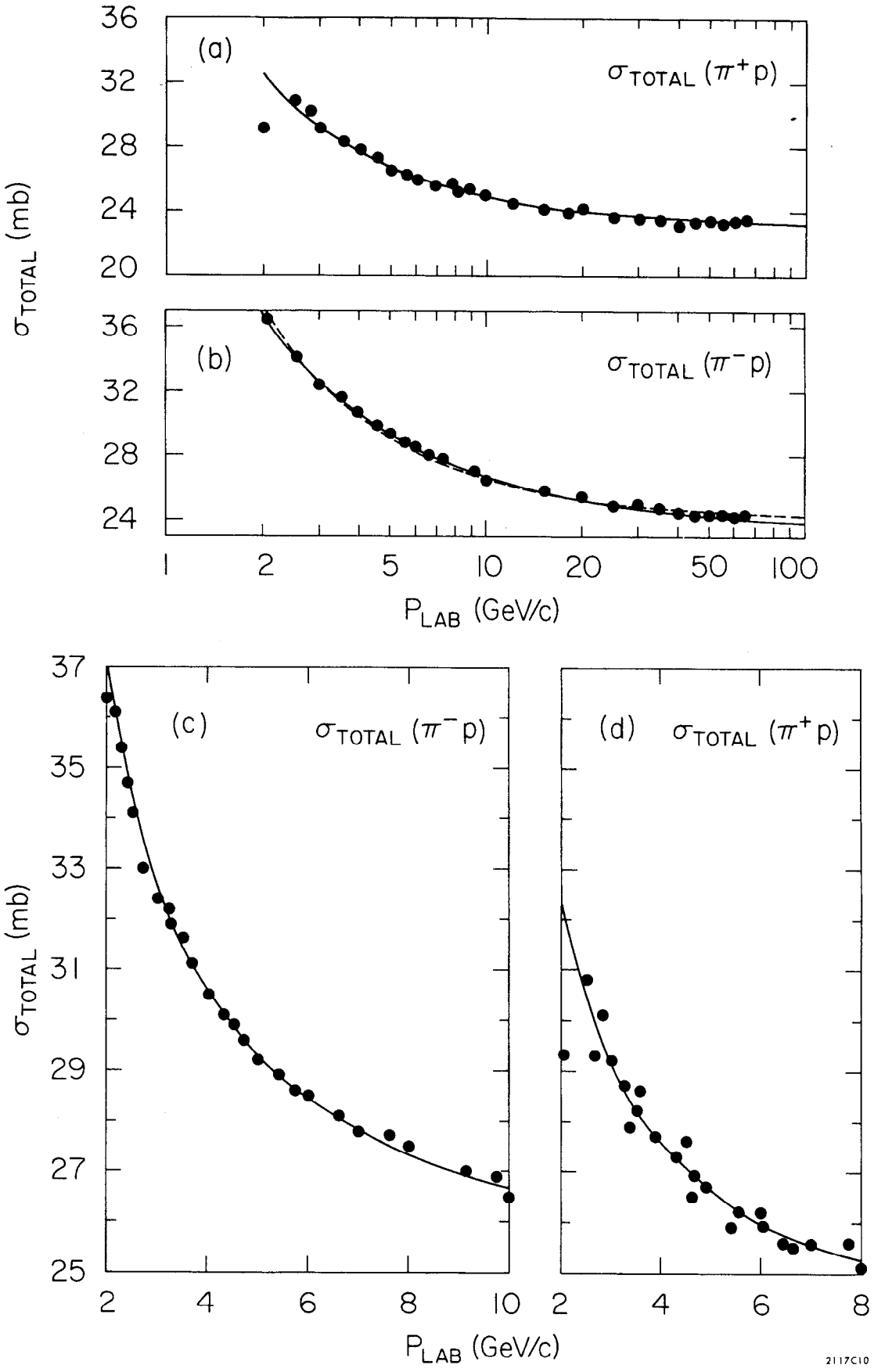
(a)
σ_{TOTAL} (π^+p)
(b)
σ_{TOTAL} (π^-p)
σ_{TOTAL} (mb)
P_{LAB} (GeV/c)
(c)
σ_{TOTAL} (π^-p)
(d)
σ_{TOTAL} (π^+p)
σ_{TOTAL} (mb)
P_{LAB} (GeV/c)
2117C10

FIG. 6

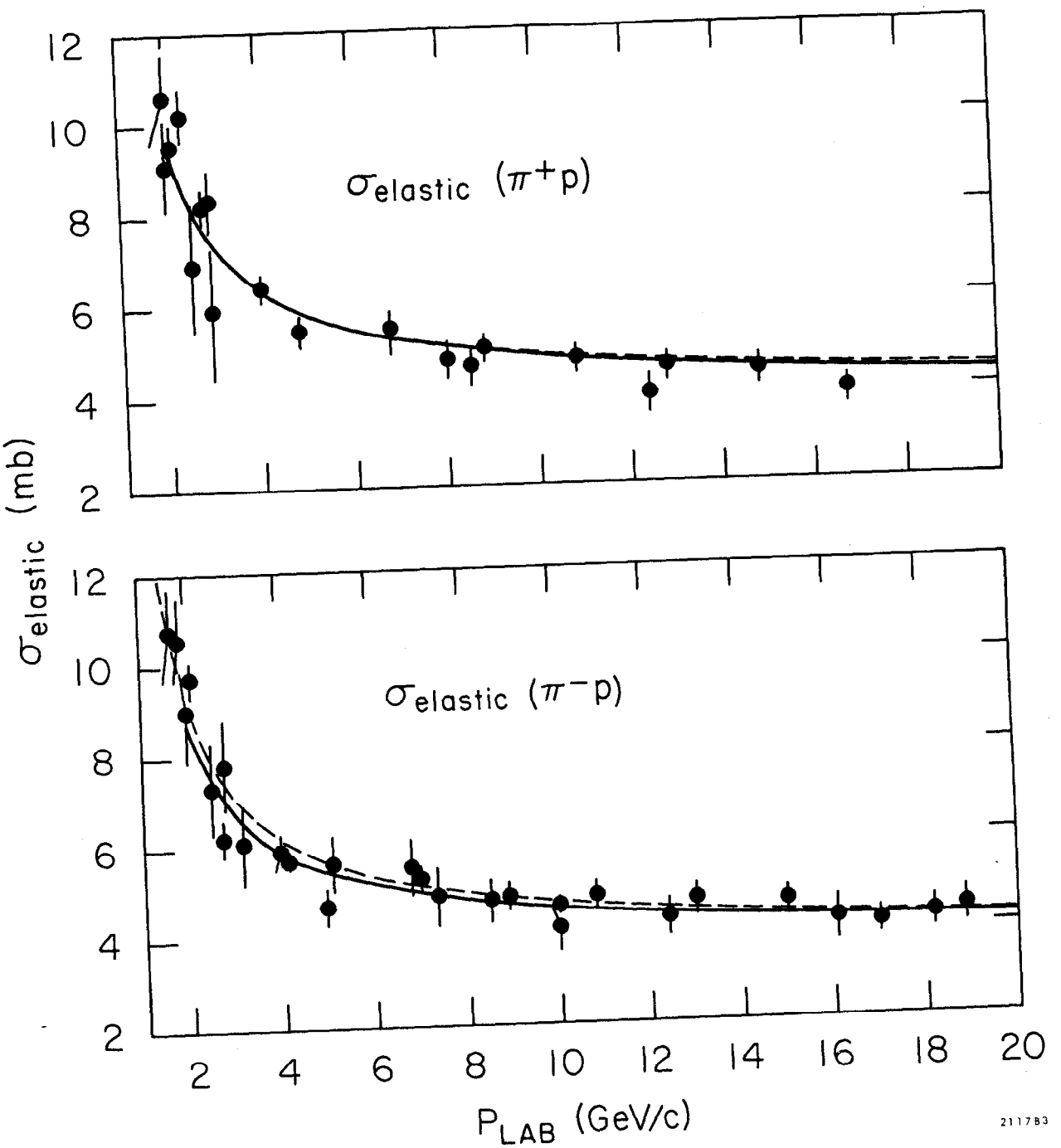
12
10
8
6
4
2
$\sigma_{elastic}$ $(\pi^+ p)$
$\sigma_{elastic}$ $(\pi^- p)$
$\sigma_{elastic}$ (mb)
2
4
6
8
10
12
14
16
18
20
P_{LAB} (GeV/c)
2117B3

FIG. 7

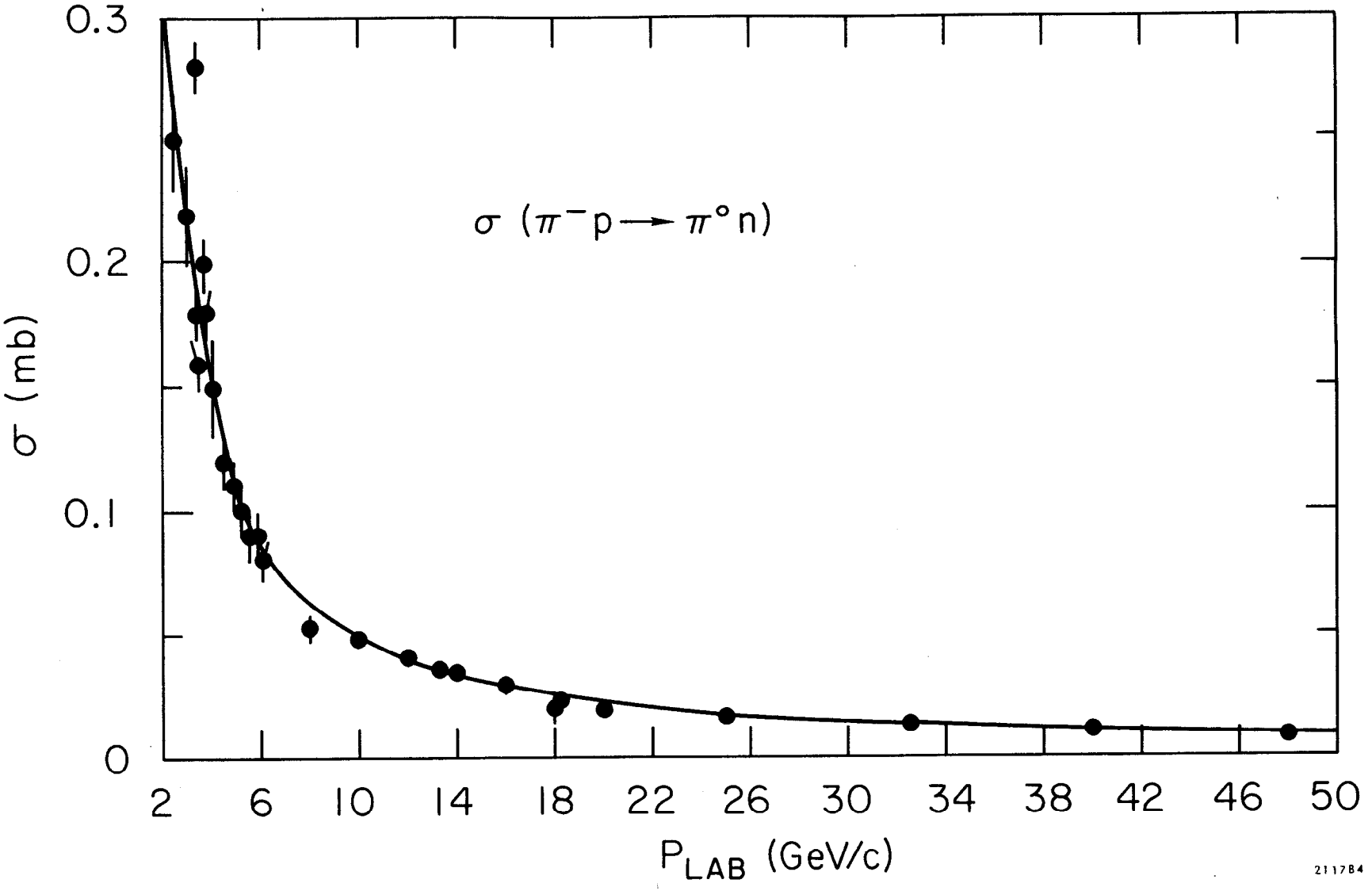
0.3
0.2
0.1
0
σ (mb)
σ (π⁻p → π°n)
2
6
10
14
18
22
26
30
34
38
42
46
50
P_LAB (GeV/c)
211784

FIG. 8

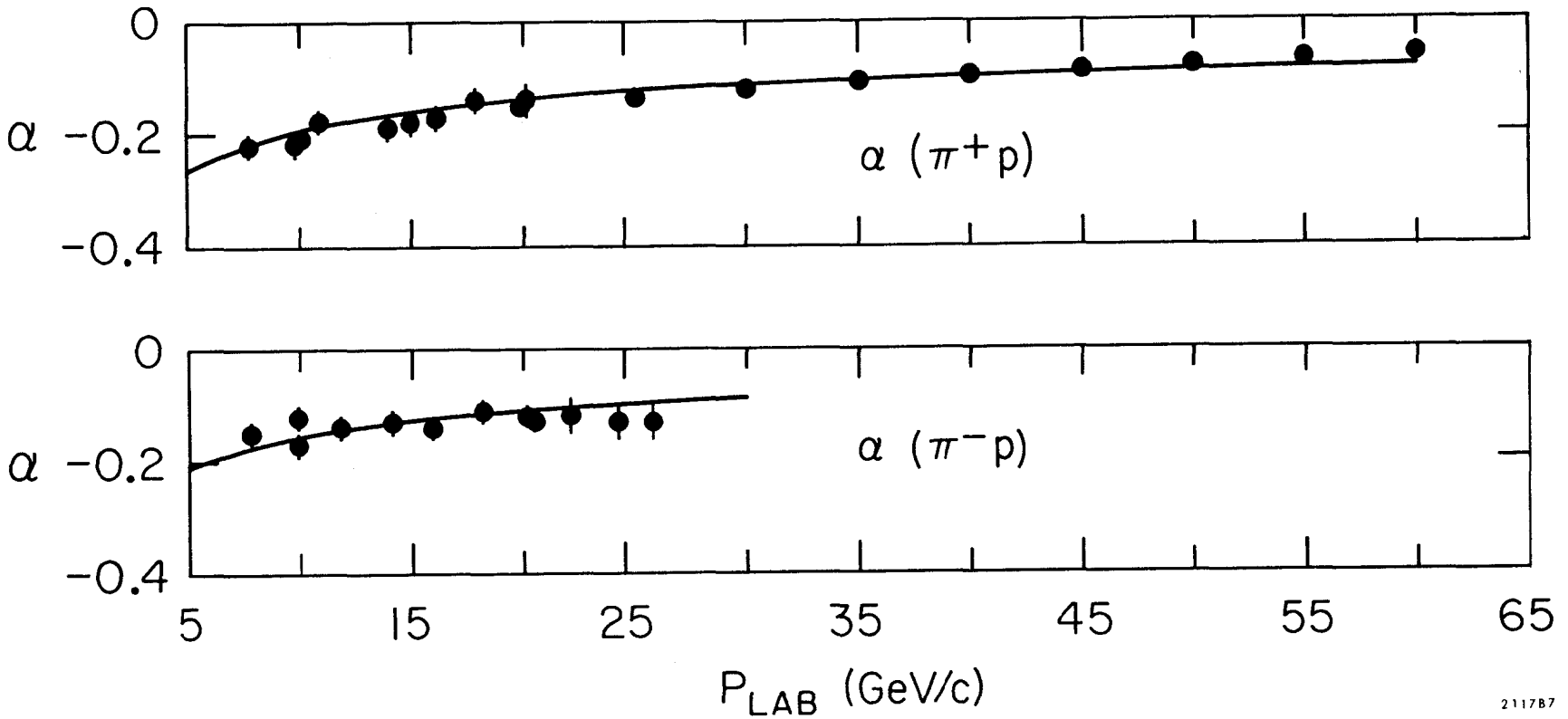

FIG. 9

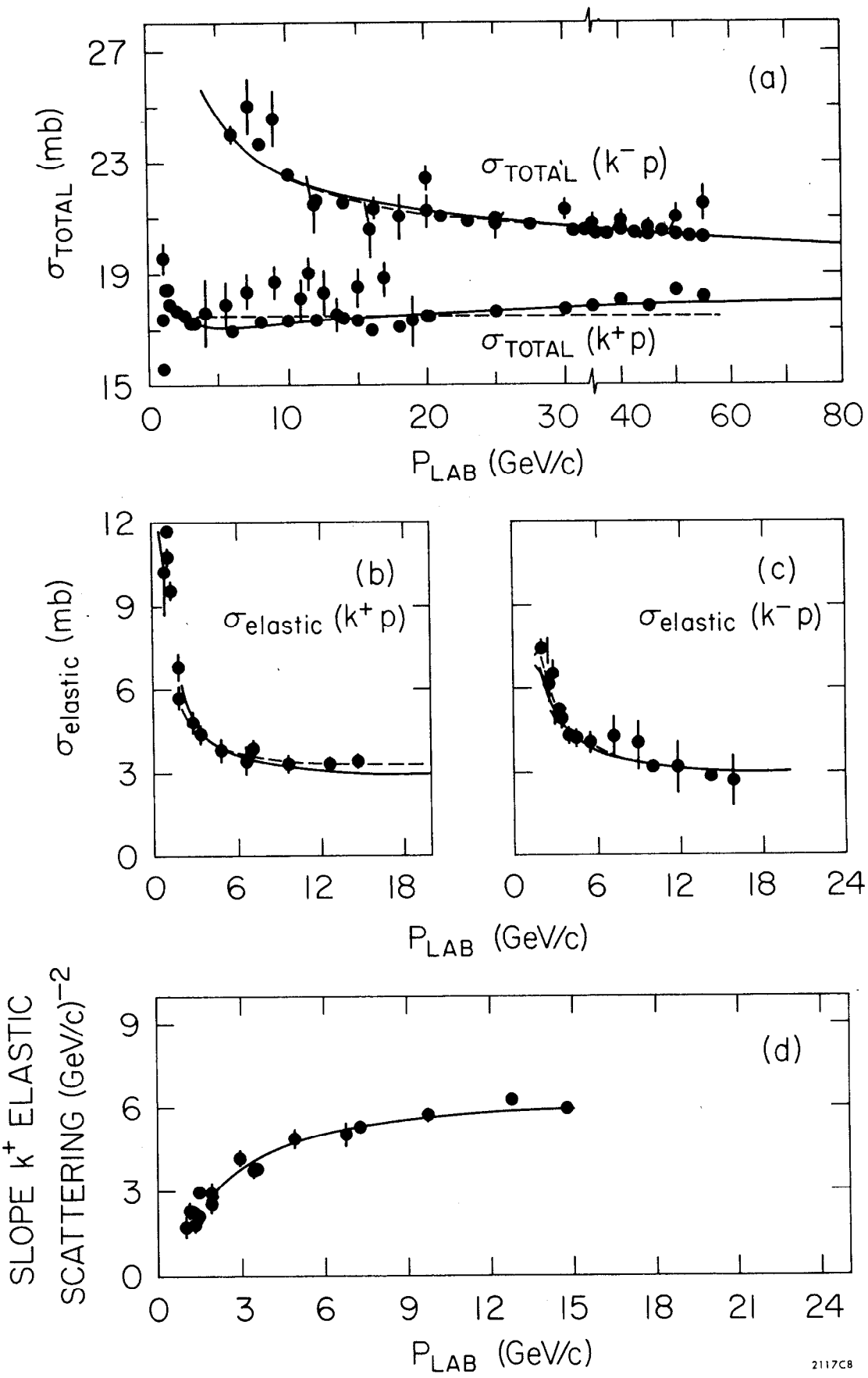
(a)
σ_{TOTAL} (mb)
σ_{TOTAL} ($k^- p$)
σ_{TOTAL} ($k^+ p$)
P_{LAB} (GeV/c)
(b)
$\sigma_{elastic}$ ($k^+ p$)
(c)
$\sigma_{elastic}$ ($k^- p$)
$\sigma_{elastic}$ (mb)
P_{LAB} (GeV/c)
(d)
SLOPE k^+ ELASTIC SCATTERING $(GeV/c)^{-2}$
P_{LAB} (GeV/c)
2117C8

FIG. 10

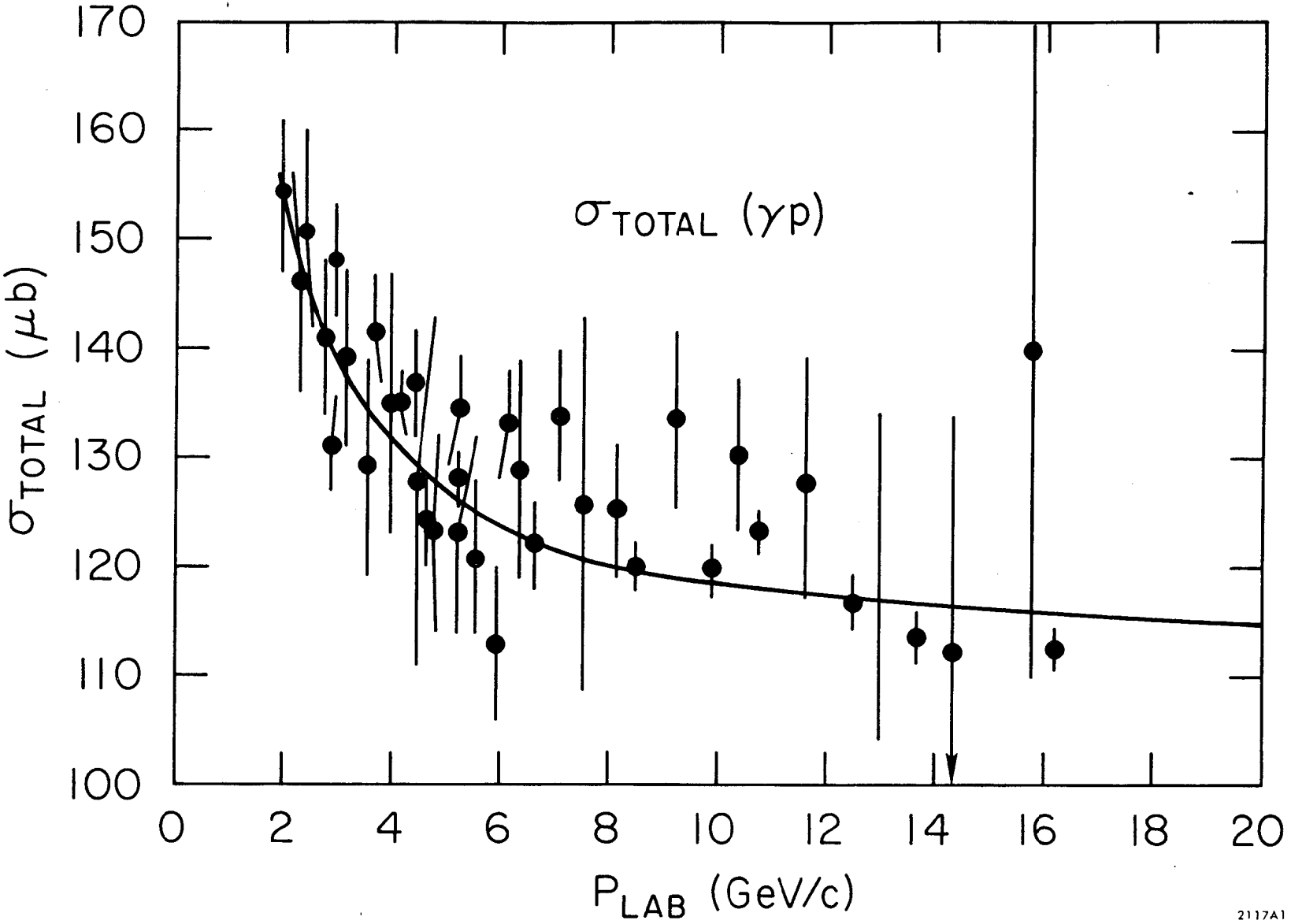
170
160
150
140
130
120
110
100
σ_{TOTAL} (μb)
σ_{TOTAL} (γp)
0
2
4
6
8
10
12
14
16
18
20
P_{LAB} (GeV/c)
2117A1

FIG. 11